



Research Journal of
**Environmental
Sciences**

ISSN 1819-3412



Academic
Journals Inc.

www.academicjournals.com

Mass Change Calculations During Hydrothermal Alteration/Mineralization in the Porphyry Copper Deposit of Darrehzar, Iran

¹R. Derakhshani and ²M. Abdolzadeh

¹Department of Geology, Shahid Bahonar University of Kerman, Kerman, Iran

²Department of Environment of Kerman Province, Havaniruz Street, Kerman, Iran

Abstract: Quantitatively evaluating of mass changes of major and minor elements that accompanied alteration in granodioritic rocks of Darrehzar porphyry copper deposit based on elements that were immobile during alteration is the aim of study that is done for the first time. Darrehzar porphyry copper deposit has four distinct types of hypogene alterations: Potassic, Phyllic, Argillic and Propylitic. Mineralogic study of these ore bodies distinguished an upper oxidation zone, an intermediate enriched zone and a primary sulfide zone. Copper mineralization was accompanied by both potassic and phyllic alterations. Supergene alteration was minor and restricted to a thin blanket of Cu sulfides under an argillic cap. Isocon plots illustrate that Al, Ti and Ga were relatively immobile during alteration and the mass was essentially conserved during alteration. At all stages in the evolution of the hydrothermal system, TiO₂ and Al₂O₃ which are immobile and have a high correlation coefficient are used in the calculations. In the potassic alteration zone there is an obvious enrichment in K and depletion in Na, Ca, Mn and Fe. These changes were due to replacement of plagioclase and amphibole by K-feldspar and biotite, respectively. Potassic alteration was associated with a large increase in Cu represented by disseminated chalcopyrite and bornite in this zone. Phyllic alteration was accompanied by the depletion of Na, K, Fe and Ba and the enrichment of Si and Cu. The loss of Na, K and Fe reflects the sericitization of alkali feldspar and the destruction of ferromagnesian minerals. The addition of Si is consistent with widespread silicification which is a major feature of phyllic alteration and the addition Cu, mobilized from the potassic zone which is depleted in this element.

Key words: Hypogene, potassic, phyllic, argillic, propylitic, supergene

INTRODUCTION

Most of the known porphyry Copper deposits in Iran as well as Darrehzar deposit (Fig. 1) are in the Central Iranian Tectono-Volcanic Belt (Ranjbar *et al.*, 2004) where is also called Urumieh-Dokhtar magmatic assemblage (Shahabpour, 1991). This zone is aligned parallel to the Zagros Thrust Zone and also to the prevalent fold axes in the Zagros Mountain Range (Jankovic, 1977; Amidi *et al.*, 1984). The magmatic processes and associated mineralization in this belt are thought to be related to subduction along the Zagros Thrust Zone (Forster, 1978; Shahabpour and Kramers, 1987; Alavi, 1980, 1994; Shahabpour and Doorandish, 2008; Derakhshani and Farhoudi, 2005).

The mineralization at Darrehzar is associated with a granodiorite stock intruded into a Thrusted and folded early Tertiary Volcano-Sedimentary series comprising andesitic lava, tuffs, ignimbrites and agglomerates. The orebody contains 80 million tons of ore, with an average grade of 0.55% Cu and approximately 0.005% Mb.

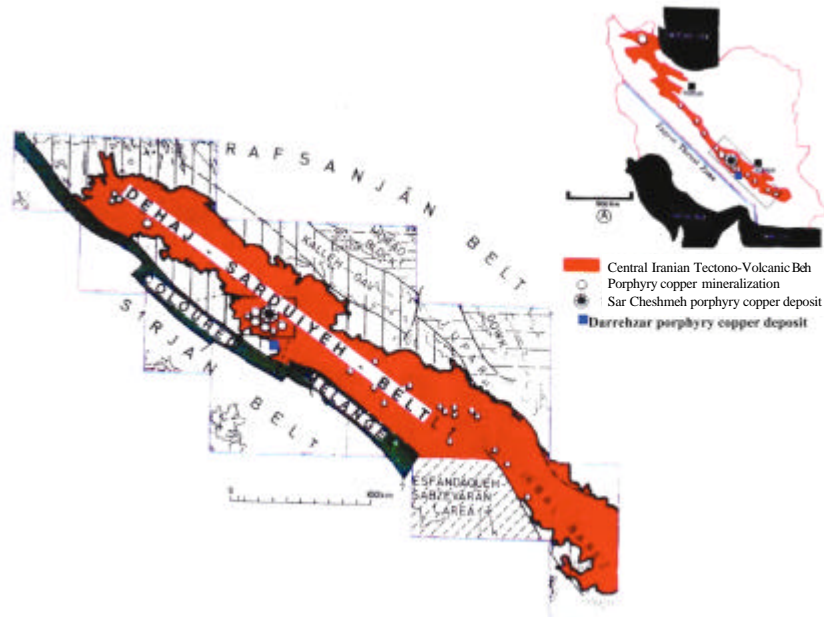


Fig. 1: Geological map of the study area

In this study, for the first time, the mass changes of major and minor elements that accompanied alteration in granodioritic rocks of the Darrehzar porphyry copper deposit is evaluated quantitatively based on elements that were immobile during alteration. The masses of components added to or removed from the rock as a result of its interaction with hydrothermal fluids are determined by comparing the corrected analyses for the altered rocks with those of least-altered equivalents.

MATERIALS AND METHODS

This study which is conducted in 2007 is concentrated on mass change calculations in the porphyry copper deposit of Darrehzar, Iran. It is considered that elements that are immobile during hydrothermal alteration and other interactive water-rock systems are concentrated during net mass loss and diluted by net mass gain. Calculations of these changes (material changes) requires different approaches when the altered rocks are derived from one, or more parent rock (single or multiple precursor). In single precursor systems the changes are calculated as displacements from a uniform rock composition. In this system, residual concentration and dilution of immobile elements produce linear arrays of data on binary diagrams that contain the precursor composition and extrapolate to the origin. Element having chemical affinity must be avoided in such tests because of unaltered correlation. Mass changes are calculated from the concentration ratio of an immobile element in an altered samples and its precursor. The method of mass changes (Grant, 1986; Maclean, 1988) was used to show that Al, Ti, Zr, Nb and Yb were highly immobile in the alteration zone of Darrehzar porphyry copper. These tests have shown that Al and Ti were extremely immobile during hydrothermal alteration of intrusive rocks.

The best fit line to binary plot of magmatic incompatible elements passes through the origin. If these elements are immobile during alteration, addition of other material (as in silicification) dilutes their concentration and they plot closer to the origin, whereas extraction of material (as by solution)

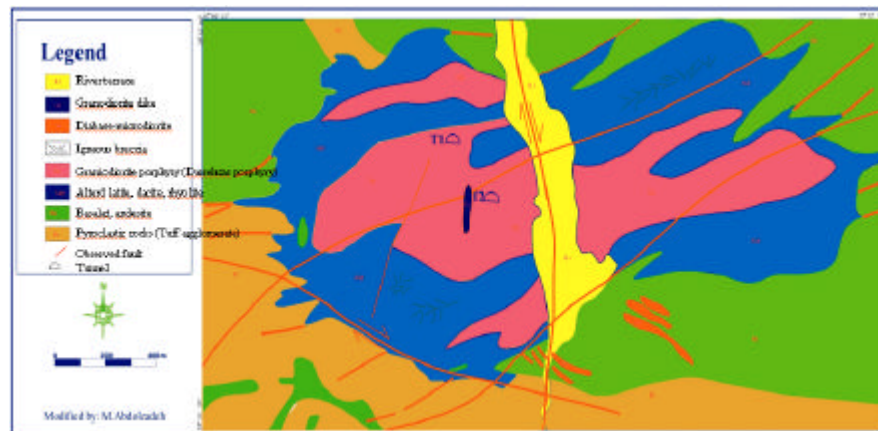


Fig. 2: Geological map of Darrehzar deposit and its major faults

concentrates them and they plot farther away from the origin. Thus, immobile incompatible elements in both fresh and altered rocks plot on a common regression line, that is, they retain constant interelement ratios.

Geology of Darrehzar Area

Darrehzar is located in Southwestern Iran (~70 km Southwest of Kerman city) and is associated with an Oligocene granodiorite that intrudes an Eocene volcanic sedimentary complex comprised mainly of volcanic-classic andesite, trachyandesite and sedimentary rocks. Dykes of quartz-microdiorite, microdiorite and granodiorite intrude the volcanic sedimentary complex in the southern part of area (Fig. 2).

The central part of Darrehzar area is composed of intensively hydrothermal altered rocks, covering the surface of about 1.8 km². Altered zone is elongated in east-west direction, longer axis has about 2.2 km length, where the shorter one is about 1 km. Boundary between the altered and unaltered rocks, is almost sharp and clear. These alterations are better developed in the western part of the area, while to the south the rocks are less altered. The fresh rocks are sometimes embraced by the altered ones. Hydrothermal alteration is very intensive as well as Sarcheshmeh one (Hezarkhani, 2006). Additional weathering changed them even more, so that, even in thin section it is often impossible to determine the kind of rock. Granodiorite porphyries are situated in the central part of alteration zone. Propylitic and Phyllic alterations are pervasive in the surface rocks (Ranjbar *et al.*, 2001) with sporadic small area of argillic alteration. However, Argillic alteration is difficult to distinguish from supergene weathering of the primary alteration type. In order to improve resolution of such areas, integration of remote sensing and geophysical data may be helpful (Honarmand *et al.*, 2002).

PETROGRAPHY

The Darrehzar stock is a complex intrusive body, mainly highly altered granodiorite, which crop out over an area of about 1 by 2.2 km.

Petrographic observations of thin sections indicate that granodiorite rock contains 50 to 65% phenocrysts including zonal plagioclase, highly altered hornblende, quartz and biotite. Hornblende was the earliest major mineral to crystallize and forms euhedral to subhedral phenocrysts. Quartz phenocrysts crystallized next and are ubiquitously rounded or embayed. Plagioclase phenocrysts

(mainly subhedral) formed shortly after the quartz phenocrysts and biotite phenocrysts (subhedral to anhedral) formed late. The granodiorite groundmass is fine grained and consists mainly of quartz, plagioclase and K-feldspar, with lesser biotite and amphibole. Apatite, zircon, titanite and rutile are present in minor to trace element.

Dykes consist mainly of plagioclase, K-feldspar, biotite, quartz and highly altered amphibole. Plagioclase occurs both as microcrystals in the groundmass and phenocrysts and composes more than 40% of the total volume of the rock unit. K-feldspar crystals compose up to 30 Vol. Percent of the total volume of the rock and occur both as phenocrysts and in the groundmass. Apatite, quartz and magnetite occur as inclusion in the plagioclase and K-feldspar.

The andesite is typically green-gray to brown-gray, holocrystalline and porphyritic with a fine grained matrix. It consists of essential plagioclase, orthoclase, blue-green to brown hornblende, magnetite and trace amounts of biotite, clinopyroxene, quartz, rutile, apatite and zircon.

Alteration and Mineralization

The earliest alteration is represented by potassic mineral assemblages developed pervasively and as halos around veins in the deep and central part of the Darrehzar stock (Fig. 3). Potassic alteration is characterized by K-feldspar, irregularly shape crystals of enriched biotite and anhydrite. Potassically altered rocks contain plagioclase, K-feldspar, ferromagnesian minerals (mainly biotite, sericite and chlorite) and chalcopyrite, pyrite, titanite, zircon and rutile. Igneous biotites are replaced by secondary biotites which crystallize in small subhedral flakes. This replacement is frequently located at the rims of igneous biotite. It can sometimes be complete in strongly altered samples. Some igneous biotites do not show those recrystallization features, but the presence of rutile between their cleavages and their chemistry indicate that they were affected by the potassic alteration.

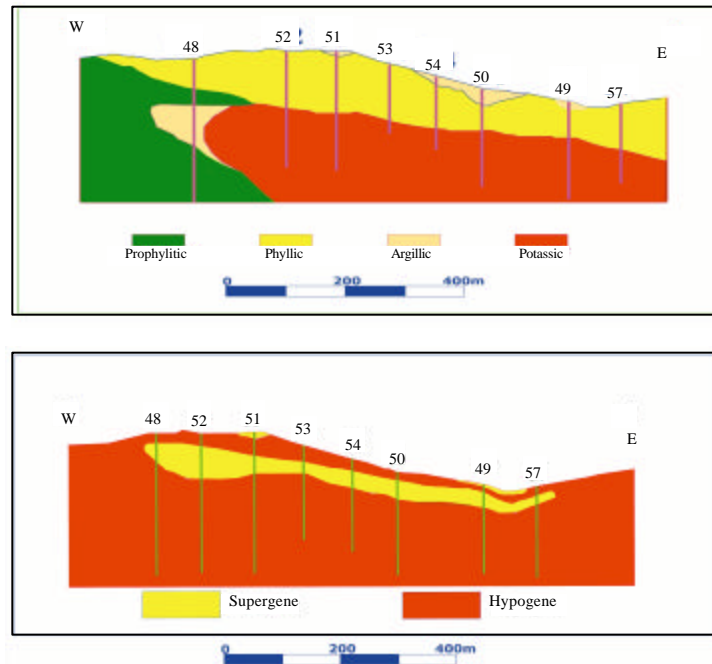


Fig. 3: Alteration profiles of the Darrehzar deposit

There is a relatively sharp boundary between the propylitic and potassic alteration zones in the deep part of the deposit. Propylitic alteration is pervasive and represented mainly by chloritization of primary and secondary biotite and groundmass material in rock peripheral to the central potassic zone. Epidote replaced plagioclase. Minor minerals associated with propylitic alteration are calcite, sericite and pyrite. The propylitic zone occurs in the peripheral parts of the system. Propylitic alteration is irregular in intensity and generally diffuses, except for some rare small epidote veinlets. The propylitic alteration zone surrounds the area of potassic alteration.

Phyllic alteration is characterized by the replacement of almost all rock-forming silicates by sericite and quartz and overprints the earlier formed potassic zone. Pyrite forms of the rock and occurs in veins and dissemination quartz veins are surrounded by chalcopyrite. Silicification was synchronous with phyllic alteration.

The argillic alteration zone is characteristic of the shallow levels of the system, where it forms a blanket over the intrusion and replaces the phyllic zone downward and the propylitic fringe laterally. Feldspar is locally altered to clay and the entire rock has been altered to assemblages of clay minerals, hematite and quartz. The affected rocks are soft and white colored. The alteration is manifested by advanced replacement of plagioclase and mafic phase by clay minerals.

Hypogene copper mineralization was introduced during potassic and to a lesser extent during phyllic alteration and exists as disseminations and in veinlet form. During potassic alteration, the copper was deposited as chalcopyrite and minor bornite. Later hypogene copper was deposited mainly as chalcopyrite. Hypogene molybdenite was concentrated mainly in the deep part of the stock and is associated exclusively with potassic alteration, where it is found in quartz veins accompanied by K-feldspar, anhydrite, sericite and lesser chalcopyrite. The concentration of sulfides and copper mineralization increase outward from the central part of the stock, with the latter generally reaching a maximum along the interface between the potassic and phyllic alteration zones and in silicified phyllically altered rocks. Sulfide concentrations, mainly pyrite are highest in the phyllic alteration zone. At the exposed surface of the deposit, rocks are highly altered and the only mineral which has survived in supergene argillization is quartz. Most of the sulfide minerals have been leached and copper was concentrated in an underlying supergene zone by downward-percolating groundwaters. This zone is very limited and consists of a thin blanket containing covellite, chalcocite and digenite located below a thin, intensely oxidized cap. The main Cu mineral in the deposit is chalcopyrite, which occurs as center line filling in quartz veins or patches between the quartz and magnetite grains of vein, i.e., petrographically late compared to most of the vein. These veins are more commonly associated with biotite-K-feldspar-quartz alteration, with very narrow alteration halos of K-feldspar. Chalcopyrite is found also disseminated in the potassic alteration and in parts of the quartz-magnetite veinlet where it is intergrown with magnetite or lies along grain boundaries between magnetite and quartz grains. Copper mineralization mainly situated in the hydrothermally altered granodiorite porphyrite rocks.

Mass Changes in Altered Zones

The least-altered granodiorite samples are typically found in the deepest part of the deposit. Three samples of these rocks were selected and compared in terms of element concentration. Most elements plot close to or on these isocons, which illustrates a very similar composition of chosen precursor samples (Table 1). Comparison of sample D36 (representative of the potassic zone) with the least-altered sample (GD) indicates that the immobile elements, Ti, Al and Ga plot close to or on the line of constant mass. However, the elements Zr and Nb, which are generally considered to be geochemically immobile, plot out of the line, possibly due to a nugget effect. As expected from the mineral assemblage in the potassic alteration zone, K and Ba as well as Cu are enriched in sample D36. By contrast Na is depleted, as well as Fe, Ca and Mn. The gains and losses of major and trace elements

Table 1: Variations in major and trace element mass changes in the fresh rock

Type No. sample	Granodiorite fresh rocks				Major element normalized to 100% for mass changes calculations				
	G1	G2	G3	GD	G1	G2	G3	GD	Average
SiO ₂ (%)	66.66	68.23	65.23	66.707	64.947	65.261	63.955	64.726	64.722
Al ₂ O ₃ (%)	15.45	15.8	16.1	15.783	15.053	15.113	15.785	15.315	15.316
Fe ₂ O ₃ (%)	4.9	4.5	4.3	4.5667	4.7741	4.3042	4.2159	4.4311	4.4313
CaO (%)	4.3	4.74	5.3	4.78	4.1895	4.5338	5.1964	4.6381	4.6394
Na ₂ O (%)	3.44	4.32	3.62	3.7933	3.3516	4.132	3.5492	3.6807	3.6784
MgO (%)	3.47	2.9	3.2	3.19	3.3808	2.7738	3.1374	3.0953	3.0968
K ₂ O (%)	2.86	2.48	2.65	2.6633	2.7865	2.3721	2.5982	2.5843	2.5853
TiO ₂ (%)	0.54	0.54	0.57	0.55	0.5261	0.5165	0.5589	0.5337	0.5338
MnO (%)	0.09	0.11	0.101	0.1003	0.0877	0.1052	0.099	0.0974	0.0973
P ₂ O ₅ (%)	0.22	0.25	0.24	0.2367	0.2143	0.2391	0.2353	0.2296	0.2296
S (%)	0.047	0.0427	0.05	0.0466	0.0458	0.0408	0.049	0.0452	0.0452
Cl	278	113	350	278	278	113	350	247	247
Rb (ppm)	57	62	48	57	57	62	48	55.66	55.665
Sr (ppm)	650	720	685	650	650	720	685	685	685
V (ppm)	57	48	55	57	57	48	55	99	64.75
W (ppm)	138	141	143.5	138	138	141	143.5	140.83	140.83
Y (ppm)	19	17	20	19	19	17	20	18.7	18.675
Zr (ppm)	105	108	99	105	105	108	99	104	104
Zn (ppm)	52	33	27	52	52	33	27	37.3	37.325
Mo (ppm)	6	6	8	6	6	6	8	6.6	6.65
Ba (ppm)	395	640	531	395	395	640	531	522	522
Ce (ppm)	58	65	82	58	58	65	82	68.3	68.325
La (ppm)	25	33	29	25	25	33	29	29	29
Ga (ppm)	17	19	18	17	17	19	18	18	18
Co (ppm)	15	19	23	15	15	19	23	19	19
Cr (ppm)	15	6	12	15	15	6	12	11	11
Cu (ppm)	72	95	214	72	72	95	214	127	127
Nb (ppm)	8	13	5.4	8	8	13	5.4	8.8	8.8
Ni (ppm)	24	29	38	24	24	29	38	30.3	30.325
Pb (ppm)	9	14	16	9	9	14	16	13	13
U (ppm)	3.1	2.4	2	3.1	3.1	2.4	2	2.5	2.5
Th (ppm)	9	11	12	9	9	11	12	10.6	10.65

for selected samples are shown graphically in Fig. 5. Pair of least altered porphyry (sample GD) and K-feldspar-biotite alterations indicate strong gain in K, Si, S, Ba and Cu and lose of Na, Ca and Sr during potassic alteration (Table 2). During the consumption of hornblende and plagioclase, Ca and probably Sr are removed and Mg is essentially conserved in the replacement of chain silicates to biotite. The large amount of Ca that was probably removed from the potassic zone may contribute to the addition of calcite and epidote in the surrounding propylitic zone. Ti is assumed to be immobile and occurs as titanite in the unaltered as well as the altered samples.

The phyllic alteration zone is characterized by the presence of the large proportions of sericite and pyrite and near absence of biotite and K-feldspar. Phyllic alteration has strongly overprinted earlier potassic alteration. Comparison of potassically altered sample (D36) and representative sample of (D2) for phyllic alteration shows that the immobile elements Al and Ti plot close to or on the line (Fig. 4) of constant mass. However, Zr and Nb, which are typically immobile, plot on the line, possibly as discussed earlier, to a nugget effect. The most important mass changes in the phyllic alteration zone relative to potassically altered rock are strong depletion of Na and Ba, moderate depletion of K, Fe and Rb and addition of Ca, Mg, Mn, SiO₂ and Cu. The gains and losses of major and trace element for the selected samples pairs are shown in Fig. 5.

Comparison of sample (D3) with least-altered sample (GD) shows in Table 3. Phyllic alteration generally leads to loss of Mg, Na, Ba and addition of Cu, Pb, Rb and S. K and Si gained for this sample pair, like variations in Cu concentration, are probably dominated by variable degrees of preceding potassic alteration.

Table 2: Major and trace element mass changes at the Darrehzar deposit in potassic alteration versus the least-altered sample (GD)

Type No. sample	Potassic alteration			Major element normalized to 100% for mass changes calculation			Mass changes in the potassic alteration zone			
	D34	D35	D36	D34	D35	D36	D34	D35	D36	Average
SiO ₂ (%)	59.78	61.37	62.75	65.53	65.07	65.80	1.73	13.25	3.61	6.19
Al ₂ O ₃ (%)	15.60	16.25	16.29	17.10	17.23	17.08	2.02	5.33	2.42	3.25
Fe ₂ O ₃ (%)	3.70	3.98	3.80	4.0563	4.2201	3.985	-0.317	0.6261	-0.292	0.005
CaO (%)	2.15	2.73	2.45	2.35	2.89	2.56	-2.24	-1.16	-1.96	-1.79
Na ₂ O (%)	2.42	2.59	2.59	2.65	2.74	2.71	-0.99	-0.38	-0.85	-0.74
MgO (%)	1.65	2.15	1.95	1.80	2.27	2.04	-1.26	-0.36	-0.97	-0.86
K ₂ O (%)	3.12	3.42	3.57	3.42	3.62	3.74	0.88	1.76	1.30	1.31
TiO ₂ (%)	0.48	0.42	0.49	0.52	0.44	0.51	0.00	0.00	0.00	0.00
MnO (%)	0.04	0.05	0.05	0.04	0.05	0.05	-0.05	-0.03	-0.04	-0.04
P ₂ O ₅ (%)	0.24	0.22	0.23	0.26	0.23	0.24	0.03	0.04	0.02	0.03
S (%)	2.03	1.13	1.18	2.23	1.19	1.24	2.21	1.39	1.24	1.61
Cl (ppm)	241.80	142.60	135.60	241.80	142.60	135.60	-1.71	-76.09	-106.10	-61.30
Rb (ppm)	83.55	87.80	86.02	83.55	87.80	86.02	29.07	49.55	33.67	37.43
Sr (ppm)	520.00	480.00	450.00	520.00	480.00	450.00	-126.30	-109.70	-145.70	-127.00
V (ppm)	75.70	82.13	82.63	75.70	82.13	82.63	-22.22	-0.57	-13.18	-12.00
W (ppm)	75.70	245.00	85.40	75.70	245.00	85.40	-64.05	152.70	-52.13	12.17
Y (ppm)	17.61	15.70	14.89	17.61	15.70	14.89	-0.84	0.11	-3.23	-1.32
Zr (ppm)	134.00	125.30	100.30	134.00	125.30	100.30	31.89	46.15	0.16	26.07
Zn (ppm)	23.80	38.03	27.32	23.80	38.03	27.32	-13.16	8.27	-8.92	-4.60
Mo (ppm)	8.00	7.30	9.50	8.00	7.30	9.50	1.51	2.14	3.26	2.30
Ba (ppm)	986.60	1050.30	650.00	986.60	1050.30	650.00	478.60	736.60	153.06	456.10
Ce (ppm)	79.65	85.60	123.60	79.65	85.60	123.65	12.47	34.27	60.11	35.62
La (ppm)	23.76	24.84	41.50	23.76	24.84	41.50	-4.90	0.76	14.10	3.32
Ga (ppm)	18.11	18.82	17.49	18.11	18.82	17.49	0.36	4.55	0.16	1.69
Co (ppm)	22.03	4.91	9.20	22.03	4.91	9.20	3.34	-13.11	-9.44	-6.40
Cr (ppm)	67.20	99.88	114.50	67.20	99.88	114.51	57.15	108.69	107.92	91.25
Cu (ppm)	2195.50	879.20	891.70	2195.60	879.21	891.79	2099.60	926.60	799.10	1275.10
Nb (ppm)	12.71	10.91	20.22	12.71	10.91	20.22	4.08	4.27	12.19	6.84
Ni (ppm)	39.65	70.31	29.60	39.65	70.31	29.60	9.91	53.95	0.44	21.43
Pb (ppm)	17.15	26.21	21.68	17.15	26.21	21.68	4.39	18.40	9.51	10.77
U (ppm)	2.45	4.09	2.90	2.45	4.09	2.90	-0.01	2.40	0.51	0.96
Th (ppm)	20.26	17.41	23.12	20.26	17.41	23.12	9.94	10.26	13.41	11.20

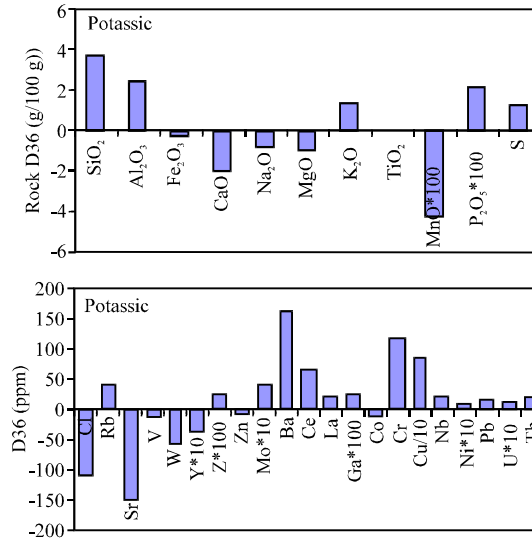


Fig. 4: Gains and losses of major and trace elements for the potassic alteration assemblage

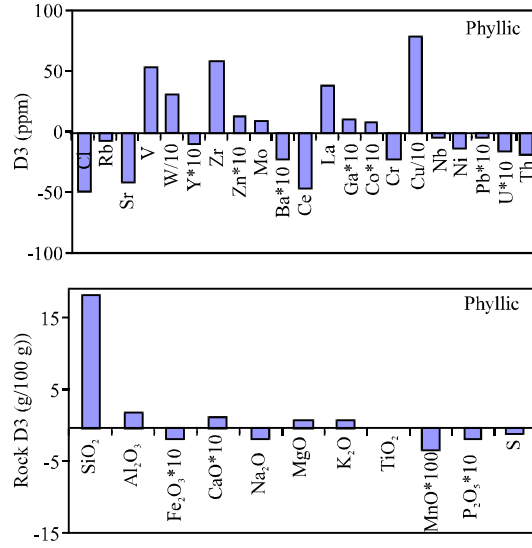


Fig. 5: Gains and losses of major and trace elements for the phyllic alteration assemblages

Table 3: Major and trace element mass changes at the Darrehzar deposit in phyllic alteration versus the least-altered sample (GD)

Type No. sample	Phyllic alteration			Major element normalized to 100% for mass changes calculation			Mass changes in the phyllic alteration zone			Average
	D1	D2	D3	D1	D2	D3	D1	D2	D3	
SiO ₂ (%)	70.35	64.30	72.30	73.63	68.08	70.30	7.47	6.76	22.96	12.40
Al ₂ O ₃ (%)	15.23	16.30	16.30	15.94	17.25	15.851	0.31	2.80	4.45	2.52
Fe ₂ O ₃ (%)	3.20	3.50	3.30	3.34	3.70	3.20	-1.14	-0.53	-0.42	-0.70
CaO (%)	1.50	1.56	2.30	1.57	1.65	2.23	-3.09	-2.90	-1.84	-2.61
Na ₂ O (%)	0.46	0.30	1.25	0.48	0.31	1.21	-3.20	-3.34	-2.16	-2.90
MgO (%)	1.30	5.23	2.51	1.36	5.53	2.44	-1.76	2.71	-0.05	0.30
K ₂ O (%)	2.65	2.17	3.97	2.77	2.29	3.86	0.13	-0.17	2.23	0.73
TiO ₂ (%)	0.52	0.48	0.44	0.54	0.50	0.42	0.00	0.00	0.00	0.00
MnO (%)	0.00	0.01	0.02	0.00	0.01	0.01	-0.09	-0.086	-0.073	-0.083
P ₂ O ₅ (%)	0.24	0.20	0.08	0.25	0.21	0.07	0.01	-0.007	-0.13	-0.04
S (%)	0.088	0.393	0.363	0.09	0.41	0.35	0.04	0.39	0.39	0.27
Cl (ppm)	25.41	57.47	73.560	25.41	57.47	73.56	-222.10	-186.70	-155.30	-188.00
Rb (ppm)	101.95	74.72	72.90	101.95	74.72	72.90	44.30	22.79	35.26	34.12
Sr (ppm)	194.09	184.50	342.01	194.09	184.50	342.01	-494.60	-491.20	-258.40	-415.00
V (ppm)	65.30	116.30	112.28	65.30	116.30	112.28	-34.97	23.11	41.04	9.72
W (ppm)	256.00	125.00	321.00	256.00	125.00	321.00	110.17	-9.57	259.50	120.00
Y (ppm)	12.65	14.45	11.69	12.65	14.45	11.69	-6.29	-3.52	-4.11	-4.64
Zr (ppm)	112.34	113.76	131.45	112.34	113.76	131.45	6.149	15.45	59.95	27.18
Zn (ppm)	29.61	28.00	27.00	29.61	28.00	27.00	-8.26	-7.89	-3.62	-6.59
Mo (ppm)	5.00	23.00	15.00	5.00	23.00	15.00	-1.69	17.55	12.10	9.32
Ba (ppm)	284.00	310.00	370.00	284.00	310.00	370.00	-243.50	-196.50	-60.51	-166.80
Ce (ppm)	56.30	75.30	65.00	56.30	75.30	65.00	-13.09	10.76	12.772	15.69
La (ppm)	33.62	25.30	65.43	33.62	25.30	65.43	3.96	-2.43	52.60	18.04
Ga (ppm)	17.76	21.08	15.39	17.76	21.08	15.39	-0.58	4.13	1.19	1.58
Co (ppm)	21.61	11.52	18.23	21.61	11.52	18.23	2.18	-6.90	3.73	-0.33
Cr (ppm)	112.99	84.53	77.97	112.99	84.53	77.97	99.78	77.75	86.24	87.92
Cu (ppm)	720.00	890.00	750.00	720.00	890.00	750.00	578.90	807.50	808.40	731.60
Nb (ppm)	14.25	10.10	14.23	14.25	10.10	14.23	5.17	1.80	8.94	5.30
Ni (ppm)	21.10	34.49	25.47	21.10	34.49	25.47	-9.61	5.91	1.46	-0.75
Pb (ppm)	15.30	12.80	17.83	15.30	12.80	17.83	2.001	0.44	9.23	3.89
U (ppm)	5.25	1.00	1.20	5.25	1.00	1.20	2.64	-1.44	-1.00	0.06
Th (ppm)	5.06	6.50	4.74	5.06	6.50	4.74	-5.63	-3.77	-4.68	-4.69

Table 4: Major and trace element mass changes at the Darrehzar deposit in propylitic alteration versus the least-altered sample (GD)

Type No. sample	Propylitic alteration			Major element normalized to 100% for mass changes calculation			Mass changes in the propylitic alteration zone			
	D7	D8	D12	D7	D8	D12	D7	D8	D12	Average
SiO ₂ (%)	59.80	57.80	58.20	65.37	63.84	64.13	0.40	-4.24	-0.01	-1.28
Al ₂ O ₃ (%)	13.70	14.00	13.90	14.97	15.46	15.31	-0.39	-0.66	0.13	-0.31
Fe ₂ O ₃ (%)	3.80	4.10	4.20	4.15	4.52	4.62	-0.29	-0.14	0.23	-0.07
CaO (%)	3.45	3.70	3.54	3.77	4.08	3.90	-0.88	-0.76	-0.70	-0.78
Na ₂ O (%)	3.40	2.98	3.10	3.71	3.29	3.41	0.02	-0.56	-0.23	-0.26
MgO (%)	3.49	3.45	4.60	3.81	3.81	5.06	0.70	0.51	2.01	1.07
K ₂ O (%)	1.87	2.05	1.37	2.04	2.26	1.50	-0.54	-0.43	-1.06	-0.68
TiO ₂ (%)	0.49	0.51	0.48	0.53	0.56	0.52	0.00	0.00	0.00	0.00
MnO (%)	1.23	1.64	1.05	1.34	1.81	1.15	1.24	1.61	1.07	1.30
P ₂ O ₅ (%)	0.22	0.25	0.28	0.24	0.27	0.30	0.009	0.03	0.08	0.04
S (%)	0.028	0.045	0.029	0.03	0.04	0.03	-0.01	0.0019	-0.01	-0.01
Cl (ppm)	320.00	410.00	297.46	320.00	410.00	297.46	71.81	141.30	53.12	88.74
Rb (ppm)	55.84	53.13	52.76	55.84	53.13	52.76	-0.02	-5.33	-2.42	-2.59
Sr (ppm)	750.00	780.00	820.00	750.00	780.00	820.00	62.23	53.86	142.34	86.14
V (ppm)	60.00	70.00	65.00	60.00	70.00	65.00	-39.22	-32.69	-33.42	-35.11
W (ppm)	45.00	49.00	64.00	45.00	49.00	64.00	-96.00	-94.41	-76.25	-88.90
Y (ppm)	20.69	28.13	23.65	20.69	28.13	23.65	1.91	7.94	5.16	5.00
Zr (ppm)	164.30	156.30	167.84	164.30	156.30	167.84	59.69	44.05	65.34	56.36
Zn (ppm)	89.30	56.32	56.50	89.30	56.32	56.50	51.67	16.04	19.70	29.14
Mo (ppm)	5.60	4.80	4.30	5.60	4.80	4.30	-1.02	-2.05	-2.26	-1.78
Ba (ppm)	610.30	562.30	586.30	610.30	562.30	586.30	86.04	10.64	69.55	55.41
Ce (ppm)	69.50	74.20	69.54	69.50	74.20	69.54	0.94	1.98	1.86	1.59
La (ppm)	31.75	29.60	31.02	31.75	29.60	31.02	2.63	-0.96	2.29	1.32
Ga (ppm)	17.70	18.25	19.45	17.70	18.25	19.45	-0.36	-0.71	1.62	0.183
Co (ppm)	25.30	24.29	18.70	25.30	24.29	18.70	6.20	4.10	-0.13	3.39
Cr (ppm)	12.00	13.00	9.00	12.00	13.00	9.00	0.9557	1.3144	-1.919	0.1169
Cu (ppm)	250.00	420.00	320.00	250.00	420.00	320.00	122.07	270.80	195.80	196.20
Nb (ppm)	23.20	24.10	30.20	23.20	24.10	30.20	14.31	14.00	21.67	16.66
Ni (ppm)	98.20	65.30	75.32	98.20	65.30	75.32	67.53	31.55	45.69	48.26
Pb (ppm)	16.35	25.30	37.94	16.35	25.30	37.94	3.28	10.96	25.28	13.17
U (ppm)	2.30	1.20	1.00	2.30	1.20	1.00	-0.208	-1.36	-1.49	-1.02
Th (ppm)	11.00	11.32	12.00	11.00	11.32	12.00	0.35	0.12	1.50	0.65

In general, the propylitic alteration at the fringe of the deposit is characterized by enrichment in CO₂ and Ca, where some of which have been directly transferred from the Ca-depleted potassic zone. However, the chlorite-epidote altered Darrehzar (sample D12) in Comparison with least-altered sample (GD), only show a minor increase in Ca but is enriched in many other elements (Table 4). Particularly Zn, Pb, Mn, Sr and Ba are enriched, whereas Si and Rb are commonly depleted. The depletion in Na and K is due to the breakdown of plagioclase (Fig. 5).

Propylitic alteration generally leads to loss of K₂O, Na, Ba and some Rb and gain of Ca, Mg, Zn and Mn for this sample pair. However, the same elements also depend on the amount of clay minerals, calcite and gypsum in the sample, respectively (Fig. 5).

DISCUSSION

The alteration zone sequence and the distribution copper mineralization at the Darrehzar intrusive complex fit in the comprehensive model for porphyry copper system proposed by Hezarkhani and Jones (1998) and Ulrich and Gonthier (2001). However, the granodiorite composition of the ore-related intrusive rocks must have played a role in the evolution of this system, producing some departure from this model. The most striking difference in the alteration-mineralization pattern is the stability of

biotite rather than K-feldspar in the potassic alteration assemblage. The K-feldspar occurrence is, in fact, limited to early veinlet which crosscut plagioclase phenocrysts and to thin rims around the latter, it has never been observed in the groundmass.

Sulfide mineralization in Darrehzar porphyry is ultimately linked to the process of hydrothermal alteration as shown by the spatial and genetic association and alteration occurred in two stages. The first stage is represented by the deposition of disseminated pyrite and minor amount of chalcopyrite and sphalerite in the pyrite-quartz-feldspar porphyry. This mode of mineralization is a result of the passage of an aqueous fluid through the rocks, leading to the exchange of components between the fluid and the rock. The second stage was mainly localized along fractures and is characterized by alteration assemblages and sulfide minerals.

In the potassic alteration zone, the principal chemical changes were the enrichment of K and Ba and the depletion of Na, Ca, Mg, Mn and Fe. Mineralogically, these changes were accommodated by crystallization of K-feldspar and biotite at the expense of plagioclase and amphibole. The replacement of plagioclase and amphibole by K-feldspar and biotite, respectively, served to add K and remove Ca and Na. Depletion of Fe was due to the alteration of Fe-rich magmatic amphibole and biotite and phengitic muscovite with appreciably lower Fe/Fe+Mg ratios.

Barite was not found in the Darrehzar deposit and the only minerals that could accommodate Ba, are K-feldspar and mica, which formed in potassically altered rocks. Copper added to potassically altered rock in significant amount, as might be expected from the dissemination of chalcopyrite and bornite in this zone.

Phyllic alteration is superimposed on the potassic zone and is characterized by sericitization of feldspar. Compared to the potassic alteration zone, the phyllic alteration zone is depleted in Na, K, Fe and Ba and enriched of alkali feldspar and ferromagnesian minerals (e.g., hydrothermal biotite which had been formed during the potassic alteration), respectively. The addition of Si is consistent with the widespread silicification which is a major feature of phyllic alteration.

CONCLUSION

- The mass-balance data indicate that potassic alteration involves an exchange of K for Na and Ca plus strong hydration of the rocks
- Propylitic alteration causing the addition of Ca and the removal of SiO₂
- In the potassic alteration zone, changes in major elements were enrichment in K and depletion in Na, Ca, Mn and Fe. These changes were due to replacement of plagioclase and amphibole by K-feldspar and biotite, respectively. Potassic alteration was associated with a large addition of Cu represented by disseminated chalcopyrite and bornite in this zone
- Phyllic alteration was accompanied by depletion in Na, K, Fe and enrichment in Si and Cu. The loss of Na, K and Fe reflects the sericitization of alkali feldspar and destruction of ferromagnesian minerals. The addition of Si is consistent with the widespread silicification which is major feature of phyllic alteration and the addition of Cu mobilized from the transition zone which is depleted in this element
- The hydrothermal alteration assemblages define concentric patterns centered on the inner part of the intrusion. These alteration zones vary from a potassic core through a well-developed phyllic shell a spot argillic zone and an outer propylitic fringe

ACKNOWLEDGMENTS

The authors would like to express their gratitude to Dr. S. Liaghat for his valuable comments. We extend our thanks to Prof. F. Moore for his useful suggestions. We are also grateful to the staff of

Shiraz University especially, Dr. M. Zare, dean of the department of earth sciences, for their close cooperation. The authors greatly appreciate the scientific comments of Dr. A. Moradian, Vice Chancellor of College of Sciences, Shahid Bahonar University and also Department of Environment of Kerman Province, which enabled us to provide this research. We appreciate the critical reading by the arbitration committee and we welcome any enlightening suggestions and insightful comments.

REFERENCES

- Alavi, M., 1980. Tectonic-stratigraphic evolution to the zagros sides of Iran. *Geology*, 8: 144-149.
- Alavi, M., 1994. Tectonic of the zagros orogenic belt of Iran. New data and interpretation. *Tectonophysics*, 229: 211-238.
- Amidi, S.M., M.H. Emami and R. Michel, 1984. Alkaline character of *Eocene volcanism* in the middle part of Iran and its geodynamic situation. *Geologischen Rundschau*, 73: 917-932.
- Derakhshani, R. and G. Farhoudi, 2005. Existence of the Oman line in the empty quarter of Saudi Arabia and its continuation in the red sea. *J. Applied Sci.*, 5: 745-752.
- Forster, H., 1978. Mesozoic-cenozoic metallogenesis in Iran. *J. Geol. Soc. London*, 135: 443-455.
- Grant, J.A., 1986. The isocon diagram-a simple solution to gresens equation for metasomatic alteration. *Econ. Geol.*, 81: 1967-1982.
- Hezarkhani, A. and A. Jones, 1998. Control of alteration and mineralization in the Sungun porphyry copper deposit, Iran: Evidence from fluid inclusions and stable isotopes. *Econ. Geol.*, 93: 651-670.
- Hezarkhani, A., 2006. Hydrothermal evolution of the Sar-Cheshmeh porphyry Cu-Mo deposit, Iran: Evidence from fluid inclusions. *J. Asian Earth Sci.*, 28: 409-422.
- Honarmand, M., H. Ranjbar and Z. Moezifar, 2002. Integration and analysis of airborne geophysics and remote sensing data of sar cheshmeh area, using directed principal component analysis. *Exploration Mining Geol.*, 11: 43-48.
- Jankovic, S., 1977. The copper deposit and geotectonic setting of tethyan eurasian metallogenic belt. *Mineralium Deposita*, 12: 37-47.
- Maclean, W.H., 1988. Rare earth elements mobility at constant inter REE ratios in the alteration zone at the phelps dodge massive sulfide deposit, Matagami, Quebec. *Mineralium Deposita*, 23: 231-238.
- Ranjbar, H., H. Hassanzadeh, M. Torbati and O. Ilaghi, 2001. Integration and analysis of airborne geophysical data of the Darrehzar area, Kerman Province, Iran, using principal component analysis. *J. Applied Geophys.*, 48: 33-41.
- Ranjbar, H., M. Honarmand and Z. Moezifar, 2004. Application of the crosta technique for porphyry copper alteration mapping, using ETM+ data in the southern part of the Iranian volcanic sedimentary belt. *J. Asian Earth Sci.*, 24: 237-243.
- Shahabpour, J. and J.D. Kramers, 1987. Lead isotope data from the sarcheshmeh porphyry copper deposit, Iran. *Mineralium Deposita*, 22: 278-281.
- Shahabpour, J., 1991. Some secondary ore formation features of the sar cheshmeh porphyry copper-molybdenum deposit, Kerman, Iran. *Mineralium Deposita*, 26: 275-280.
- Shahabpour, J. and M. Doorandish, 2008. Mine drainage water from the sar cheshmeh porphyry copper mine, Kerman, IR Iran. *Environ. Monit. Assess.*, 141: 105-120.
- Ulrich, T. and D. Gonther, 2001. The evolution of a porphyry Cu-Au deposit, based on LA-ICP-MS analysis of fluid inclusions: Bago de la Alumbrera, Argentina. *Econ. Geol.*, 96: 1743-1774.